

High-Level *ab Initio* Thermochemical Data for Halides of Chromium, Manganese, and Iron

Ida M. B. Nielsen* and Mark D. Allendorf

Sandia National Laboratories, P.O. Box 969, Livermore, California 94551

Received: October 21, 2004; In Final Form: November 18, 2004

The thermochemistry of the transition-metal fluorides and chlorides MF_n and MCl_n ($\text{M} = \text{Cr}, \text{Mn}, \text{Fe}; n = 1, 2$) has been characterized by high-level *ab initio* electronic structure methods. Geometries and harmonic vibrational frequencies were computed at the B3LYP level of theory using triple- ζ basis sets including diffuse and polarization functions. Heats of formation were computed from isogyric reaction energies at the CCSD(T) level using high-quality basis sets, including corrections for core-valence correlation and scalar relativistic effects. To investigate the possible linearity of the ground states of CrCl_2 and CrF_2 , we performed geometry optimizations for these species at the CCSD(T) level using large basis sets. In both cases, a bent (${}^5\text{B}_2$) minimum structure was located, but the bent structure is only slightly below the linear form, which was found to be a transition state. For all of the investigated halides, polynomial fits were carried out for the heat capacity and the standard enthalpy and entropy in the 300–3000 K temperature range.

1. Introduction

Thermodynamic data, including heats of formation, heat capacities, and entropies for both condensed- and gas-phase compounds, are the foundation for building accurate models of all high-temperature systems. Industrial-scale processes involve a broad range of materials, such as refractories, alloys, and pure metals, whose reactivity, stability, resistance to corrosion, and reaction or decomposition products are of fundamental interest. Often, however, the gas-phase thermodynamic data required to evaluate these aspects are unavailable. Such is the case for the transition metals of interest here. Materials containing chromium, manganese, and iron are almost ubiquitous in many high-temperature systems, but knowledge of their corresponding gas-phase thermochemistry is limited. Because experimental measurements of thermochemistry are now quite rare, the only avenue for obtaining such data in a timely manner is through theoretical approaches.

This investigation is part of a larger effort to generate reliable thermodynamic data using quantum-chemical methods for gas-phase species relevant to high-temperature processes including corrosion, combustion, waste incineration, and materials manufacturing. Data generated through this work are being made available on the World Wide Web.¹ The work described here represents a first step toward generating a database of information for the gas-phase compounds of the elements chromium, manganese, and iron. Although some of the most important problems involve oxygen, water vapor, or both, we are focusing on the lighter halides here because they provide a platform for developing and understanding the performance of computational methods. Furthermore, data for halides are often the only information available for comparison in the literature. Thus, the results reported here are an important first step in the process of developing robust computational methods that can treat a wide variety of chemical systems, including those that contain oxygen.

Although heats of formation are available in the literature for many of the chlorides and fluorides of chromium, manga-

nese, and iron, several of the values presented are not well established. The more recent experimentally obtained thermochemical data for these transition-metal halides derive from two studies. Ebbinghaus² presented $\Delta H_{f,298.15}^\circ$ values for gas-phase chromium species, including the chlorides and fluorides. The heats of formation of CrCl , CrCl_2 , CrF , and CrF_2 were computed by the third-law method using the vapor-pressure data available in the literature as well as the thermodynamic functions computed from the literature values for structures and vibrational frequencies. In another study, Hildenbrand³ determined $\Delta H_{f,298.15}^\circ$ values for MCl and MCl_2 ($\text{M} = \text{Cr}, \text{Mn}, \text{Fe}$) obtained by a mass spectrometric study of the gaseous equilibria $\text{MCl} + \text{Ag} = \text{M} + \text{AgCl}$ and $\text{M} + \text{MCl}_2 = 2\text{MCl}$ and by measurement of sublimation pressures of solid MCl_2 . Additionally, some thermochemical data for the fluorides and chlorides of Cr, Mn, and Fe are available in the JANAF⁴ and NBS tables.⁵ The available experimental thermochemical data are summarized in Table 1.

Most of the previous theoretical investigations of the thermochemistry of the halides of Cr, Mn, and Fe employ density functional theory (DFT), but a few theoretical studies use more sophisticated correlated-electronic-structure methods, including quadratic configuration interaction with single and double substitutions and a perturbative estimate for triple substitutions (QCISD(T)), multireference configuration interaction (MRCI), and the coupled-cluster singles and doubles method with a perturbative correction for connected triple substitutions (CCSD(T)). Previously computed heats of formation of the pertinent transition-metal halides are given in Table 2. The heats of formation reported in Table 2 were either taken directly from the cited sources or computed from atomization energies or bond-dissociation energies in these sources using established atomic heats of formation from the JANAF Tables.⁴

Although most of the first-row transition-metal difluorides and dichlorides have been found to be linear (see, e.g., refs 3 and 6 and references therein), there is some uncertainty regarding the shape of CrCl_2 and CrF_2 . Experimental studies of CrCl_2 have proposed either a linear or a bent structure: electron-diffraction data indicated a bent structure⁷ but were later

* Corresponding author. E-mail: ibniels@ca.sandia.gov.

TABLE 1: Experimental Values for Heats of Formation (kcal mol⁻¹) for Fluorides and Chlorides of Cr, Mn, and Fe

species	$\Delta H_{f,0}^{\circ}$	$\Delta H_{f,298.15}^{\circ}$
CrF		$4.57 \pm 2.41;^a 7.6 \pm 4^b$
CrF ₂		$-103.23 \pm 2.96;^a -98.9;^c -94.0 \pm 4^b$
CrCl		$33.7 \pm 1.6;^d 31.05 \pm 0.65^a$
CrCl ₂		$-26.3 \pm 1;^d -28.11 \pm 0.41;^a -30.7^c$
MnF	$-5.0;^c -18.2 \pm 3;^e -20.3 \pm 3^f$	$-5.2;^c -14.5 \pm 4^g$
MnF ₂	-133.2 ± 2^f	
MnCl	10.10^c	$15.8 \pm 1.6;^d 10.11^c$
MnCl ₂		$-62.6 \pm 1;^d -63.0^c$
FeF	11.36 ± 4.78^h	11.40 ± 4.78^h
FeF ₂	-92.94 ± 3.39^h	-93.10 ± 3.39^h
FeCl	$59.7 \pm 20;^h 47 \pm 3^i$	$60.0 \pm 20;^h 49.5 \pm 1.6^d$
FeCl ₂	-33.8 ± 0.5^h	$-33.7 \pm 0.5;^h -32.8 \pm 1;^d -35.5^c$

^a Reference 2. ^b Reference 37. ^c Reference 5. ^d Reference 3. ^e Reference 38. ^f Reference 39. ^g Reference 40. ^h Reference 4. ⁱ Reference 41.

TABLE 2: Heats of Formation (kcal mol⁻¹) for Fluorides and Chlorides of Cr, Mn, and Fe Obtained in Previous Theoretical Investigations

species	$\Delta H_{f,0}^{\circ}$	$\Delta H_{f,298.15}^{\circ}$
CrF	$-3.25;^a 4^b$	-3.13^a
CrF ₂	-125.29^c	
CrCl		
CrCl ₂	-29.47^c	
MnF	-19.5^b	
MnF ₂	-164.34^c	
MnCl		
MnCl ₂	-72.89^c	
FeF	$4.05;^d 14.3^g$	
FeF ₂	-136.72^c	
FeCl	$47.9;^e 41.4;^d 54.0^g$	45.3^f
FeCl ₂	-45.27^c	-35.8^f

^a Reference 27. From CCSD(T) energies computed with a (14s11p6d6f4g)/[8s7p6d4f2g] (Cr), aug-cc-pVTZ (F) basis and including a relativistic correction. ^b Computed from the bond dissociation energy (D_e) in ref 34 using our ZPVE correction; D_e was obtained at the MRCI level using an ANO [7s6p4d3f2g] set on the metal and the aug-cc-pVTZ set on F, including the Davidson correction and corrections for core-correlation and scalar relativistic effects. ^c Reference 35. Computed from atomization energies obtained at the VWN-BP DFT level with a triple- ζ plus polarization quality basis set, including a relativistic correction. ^d Reference 36. From atomization energies computed at the CCSD(T) level with a (20s15p10d6f4g)/[8s7p4d3f2g] (Fe), aug-cc-pVQZ (Cl) basis including an empirical correction based on the results obtained for CuCl. ^e Reference 42. Average of B3LYP and CCSD(T) energies computed with Stuttgart ECP,(8s7p6d2f)/[6s5p4d2f] (Fe), 6-311++G(3df,3pd) (Cl) basis. ^f Reference 43. From estimated QCISD(T) (15s11p8d3f)/[9s6p5d3f](Fe), (14s11p3d1f)/[7s6p3d1f] (Cl) energies. ^g Reference 44. From B3LYP energies computed with Stuttgart ECP, (8s7p6d2f)/[6s5p4d2f] (Fe), 6-311+G(3df,2p) (F,Cl).

reinterpreted to be consistent with a linear structure;⁶ experimental third-law entropy data were found to be consistent with a bent structure.³ Theoretical studies of the CrCl₂ potential-energy surface also do not provide any consensus on the shape of the global minimum. A study using local DFT located a linear (⁵Π_g) minimum,⁸ whereas a DFT study employing the B3LYP functional located a bent (⁵B₂) minimum for CrCl₂.⁹ In the latter case, CCSD(T) single-point energy computations at the B3LYP optimized geometry also predicted the bent form to have the lowest energy. For CrF₂, a combined analysis of gas-phase diffraction and the spectroscopic data yielded a linear equilibrium configuration,¹⁰ although the possibility of a bent structure could not be ruled out.

We have undertaken an ab initio study of the transition-metal fluorides and chlorides MF_{*n*} and MCl_{*n*} (M = Cr, Mn, Fe; *n* = 1, 2) to obtain a set of consistent, high-level ab initio values for the thermochemical parameters of these species. Geometries are optimized and harmonic vibrational frequencies are com-

puted using B3LYP density functional theory with a triple- ζ basis set including diffuse and polarization functions. For CrCl₂ and CrF₂, optimizations are also carried out at the CCSD(T) level using large basis sets to establish the shape of the ground state. Heats of formation are computed by means of the CCSD(T) method in conjunction with high-quality basis sets, including corrections for core-valence correlation and scalar relativistic effects. Finally, we compute thermodynamic data over a range of temperatures as well as polynomial coefficients in the CHEMKIN format¹¹ for use in the modeling of CVD and other high-temperature processes.

2. Computational Details

Optimum geometries and harmonic vibrational frequencies were computed at the B3LYP level using the 6-311+G(d) basis set.¹² For CrCl₂ and CrF₂, geometries and frequencies were also computed at the CCSD(T)/6-311+G(d) level. Additionally, a CCSD(T) optimization was performed for CrCl₂ with a larger basis set, using the 6-311+G(3df)¹² set on Cl and the Bauschlicher ANO set^{13,14} on Cr.

Heats of formation were computed at the CCSD(T) level of theory employing the frozen-core approximation (freezing 1s on F, 1s2s2p on Cl, and 1s2s2p3s3p on the transition metals). The Bauschlicher ANO basis set^{13,14} was used on the transition metals. For the halogen atoms, two different basis sets were employed: the aug-cc-pVQZ¹⁵⁻¹⁷ set for reactions involving monohalides and the smaller 6-311+G(3df) set for reactions involving dihalides.

The effect of inclusion of the transition metal's 3s and 3p core orbitals in the correlation procedure was computed using the cc-pVTZ basis for the halogen atoms and a modified Bauschlicher ANO set for the transition metals. The Bauschlicher ANO basis set was modified by uncontracting the outermost six s, seven p, and seven d functions. The resulting basis set for the transition metals has 146 basis functions. The computations of the core-valence corrections were performed at the MP2 level for all of the Mn and Fe species, whereas the CCSD(T) level was employed for the Cr compounds.

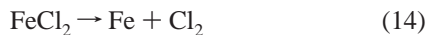
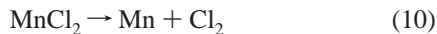
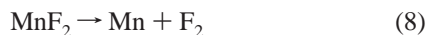
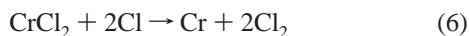
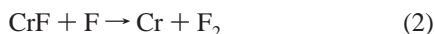
Scalar relativistic effects were accounted for using the Douglas-Kroll-Hess second-order relativistic correction¹⁸⁻²¹ at the MP2 level. For the transition metals, the Bauschlicher ANO basis was modified by decontracting the entire s and p spaces (resulting in a basis set with 124 basis functions), and for F and Cl, the cc-pVTZ_DK^{14,22} basis set was employed.

Unrestricted-reference wave functions were employed for all of the calculations involving open-shell species. The spin contamination before annihilation of the spin contaminant in the unrestricted B3LYP wave functions was less than 0.02 for all of the molecules except CrCl₂, for which a spin contamina-

tion of about 0.04 was obtained. For many of the species investigated, locating the ground state entailed doing several trial runs employing different initial guesses, obtained by computing HF or B3LYP wave functions with smaller basis sets. To ensure that the lowest electronic state was obtained, we tested the stability of the single-reference wave function, and the wave function, if pertinent, was reoptimized until it was stable (using the stable = opt keyword in the Gaussian program). For the iron compounds, the ground state is a Δ state, and the electronic state, involving partially filled degenerate orbitals, could not be determined in the full point group of the molecule. The molecular orbitals, however, were inspected to ascertain that they had the correct symmetry in the employed nondegenerate subgroup.

The large basis-set CCSD(T) optimization for CrCl_2 and the 6-311+G(d) CCSD(T) optimization for CrF_2 were performed with Molpro,²³ relativistic effects were computed with NWChem,²⁴ and the Gaussian98²⁵ and Gaussian03²⁶ programs were used for all of the other computations.

Heats of formation were computed from the following isogyric reactions:



The first reaction employed for CrF, reaction 1, is a dissociative electron attachment. As discussed previously,²⁷ this reaction benefits from the cancellation of errors because the electronic structure of the constituent chromium and fluorine atoms in CrF is similar to that of Cr and F^- . For CrCl, one of the employed reactions, reaction 4, is a dissociative electron attachment as well. For comparison, the heats of formation of CrF and CrCl were also computed from reactions 2 and 5, which involve only neutral species. For the remaining species, only one reaction was employed for each compound. In each case, an isogyric reaction was selected, in which, besides the transition-metal halide, only small species with established heats of formation appear.

Heats of formation at 298.15 K were obtained from the computed $\Delta H_{f,0}^\circ$ values by applying the thermal corrections $H_{298.15}^\circ - H_0^\circ$ obtained at the B3LYP/6-311+G(d) level of

TABLE 3: Thermochemical Data (kcal mol⁻¹) Employed in the Computation of Heats of Formation for Halides of Chromium, Manganese, and Iron^a

species	$\Delta H_{f,0}^\circ$	$\Delta H_{f,298.15}^\circ$
Cr(g)	94.49 ± 1.0	95.00
Mn(g)	67.42 ± 1.00	67.70
Fe(g)	98.73 ± 0.31	99.30
F(g)	18.74 ± 0.07	18.97 ± 0.07
F^- (g)	-59.64 ^b	-59.41
Cl(g)	28.59 ± 0.001	28.992 ± 0.002
Cl^- (g)	-54.67 ^c	-54.27

^a Unless otherwise noted, data were taken from ref 4. ^b Computed from $\Delta H_{f,0}^\circ[\text{F}]$ using the electron affinity $\text{EA}[\text{F}] = 78.38$ kcal mol⁻¹ from ref 45. ^c Computed from $\Delta H_{f,0}^\circ[\text{Cl}]$ using the electron affinity $\text{EA}[\text{Cl}] = 83.26$ kcal mol⁻¹ from ref 45.

TABLE 4: Computed Optimum Geometries, Harmonic Vibrational Frequencies, and Infrared and Raman Intensities^a

species	r_e (Å), α (deg) ^b	ω_e (cm ⁻¹) ^c
CrF (⁶ Σ^+)	1.8075	621 (167, 15)
CrF ₂ (⁵ B ₂)	1.7860, 137.5	116 (32, 2), 600 (57, 6), 701 (244, 0.2)
CrF ₂ ^d (⁵ B ₂)	1.7987, 145.1	99, 574, 748
CrCl (⁶ Σ^+)	2.2263	377 (60, 2)
CrCl ₂ (⁵ B ₂)	2.1933, 143.4	53 (16, 5), 350 (14, 15), 470 (150, 0.4)
CrCl ₂ ^d (⁵ B ₂)	2.1992, 156.2	45, 338, 486
MnF (⁷ Σ^+)	1.8521	595 (134, 8)
MnF ₂ (⁶ Σ_g)	1.8073	136 ^e (47, 0.0), 566 (0.0, 3), 714 (238, 0.0)
MnCl (⁷ Σ^+)	2.2657	361 (80, 7)
MnCl ₂ (⁶ Σ_g)	2.1983	70 ^e (21, 0.0), 324 (0.0, 8), 470 (164, 0.0)
FeF (⁶ Δ)	1.7998	631 (121, 8)
FeF ₂ (⁵ Δ)	1.7677	151 ^e (43, 0.0), 590 (0.0, 4), 741 (239, 0.0)
FeCl (⁶ Δ)	2.2072	377 (75, 8)
FeCl ₂ (⁵ Δ)	2.1524	77 ^e (17, 0.0), 338 (0.0, 10), 486 (171, 0.0)
F ₂	1.4087	982
Cl ₂	2.0533	513

^a Computed at the B3LYP/6-311+G(d) level of theory, unless otherwise noted. ^b α is the X-Cr-X (X = F, Cl) angle and is reported for the nonlinear structures. ^c After each frequency, two numbers are given in parentheses: the first is the infrared intensity (km/mol), and the second is the Raman activity (Å⁴/amu). ^d Computed at the CCSD(T)/6-311+G(d) level of theory. ^e Doubly degenerate.

theory and by using the heats of formation of the auxiliary species given in Table 3.

3. Results and Discussion

The computed optimum geometries and harmonic vibrational frequencies are listed in Table 4 along with the electronic ground state for each species. Additionally, infrared and Raman intensities, computed using the double-harmonic approximation, are included.

The B3LYP/6-311+G(d) bond distances tend to be somewhat longer than those obtained by experiment. For example, a least-squares analysis of the gas-phase electron diffraction data²⁸ yielded the values $r_e(\text{Mn}-\text{F}) = 1.797(6)$ Å for MnF₂ and $r_e(\text{Fe}-\text{F}) = 1.755(6)$ Å for FeF₂, and the computed B3LYP/6-311+G(d) bond distances of 1.807 Å (MnF₂) and 1.768 Å (FeF₂) are, thus, about 0.01 Å longer than their experimental counterparts. Likewise, for CrF and CrCl, the B3LYP/6-311+G(d) bond distances are longer than those obtained by experiment. The computed values of 1.8075 and 2.2263 Å, respectively, differ by 0.02–0.03 Å from the experimental r_e values of 1.7839 and 2.194 Å, as determined by Fourier transform spectroscopy.^{29,30}

The B3LYP/6-311+G(d) harmonic vibrational frequencies are generally lower than their experimental counterparts. For

CrF and CrCl, the computed B3LYP frequencies of 621 and 377 cm^{-1} are about 5–6% below the experimental ω_e values^{30,31} of 664.1 and 396.7 cm^{-1} . For MnF₂ and FeF₂ vibrational frequencies ν_1 – ν_3 have been reported,²⁸ viz., ν_1 , ν_2 , ν_3 = 581, 166, 746 cm^{-1} and 588, 176, 782 cm^{-1} , respectively, obtained from gas-phase electron-diffraction data. The corresponding B3LYP harmonic vibrational frequencies are somewhat lower, assuming values of 566, 136, and 714 cm^{-1} for MnF₂ and 590, 151, and 741 cm^{-1} for FeF₂.

To establish the structure of the global minimum for CrCl₂ and CrF₂, we optimized the geometries of these species at both the B3LYP and CCSD(T) levels. Using the 6-311+G(d) set, we computed the optimum geometries and harmonic vibrational frequencies, and for both CrCl₂ and CrF₂, the global minimum was found to be a bent state at both the B3LYP and CCSD(T) levels. Optimization of the linear form yielded a transition state whose imaginary frequency corresponded to the bending mode. The B3LYP frequencies, computed analytically, and the CCSD(T) frequencies, computed by finite-difference procedures using energies only (Table 4), are in fair agreement with the fundamental frequencies^{32,33} (ν_1 , ν_2 , ν_3 = 565, 155, 654 cm^{-1} for CrF₂ and 325, 110.5, 458.5 cm^{-1} for CrCl₂) obtained from inert-gas-matrix infrared and Raman spectra, assuming linear or near-linear geometries.

The linear transition state is very close to the bent minimum energetically. At the B3LYP level, the linear state lies 0.6 and 1.8 kcal mol^{-1} above the bent form for CrCl₂ and CrF₂, respectively, whereas the corresponding energy gaps at the CCSD(T) level are only 0.1 and 0.8 kcal mol^{-1} . At the CCSD(T) level, the energy difference between the linear and bent forms for CrCl₂ is, thus, below the zero-point vibrational energy for the bending mode. For the CrF₂ and CrCl₂ bent geometries, the trends observed upon going from the B3LYP to the CCSD(T) level of theory are similar. In both cases, the CCSD(T) bond distance, r_e , is longer and the bond angle, α , wider, with the changes in r_e and α being 0.013 Å, 7.3° and 0.006 Å, 12.8° for CrF₂ and CrCl₂, respectively. For CrCl₂, a CCSD(T) geometry optimization was also performed using a larger basis set, namely, the 6-311+G(3df) set on Cl and the Bauschlicher ANO basis on Cr. Frequencies were not computed at this level of theory, but a stationary point was located, corresponding to a bent structure with a Cl–Cr–Cl angle of 155.5° and a bond distance, r_e , of 2.1979 Å. The effect of improving the basis set beyond the 6-311+G(d) set at the CCSD(T) level thus appears to be very small, shortening r_e by only about 0.001 Å and narrowing the angle by less than 1°.

The computation of the heats of formation is detailed in Tables 5–7. The $\Delta H_{f,0}^\circ$ values were computed from the reaction enthalpies $\Delta H_{\text{rxn},0}^\circ$ for reactions 1–14 (which include a ZPVE correction computed from the harmonic vibrational frequencies listed in Table 4) using established heats of formation from Table 3. For example, $\Delta H_{f,0}^\circ[\text{CrF}]$ is computed from reaction 1 using the expression

$$\Delta H_{f,0}^\circ[\text{CrF}] = \Delta H_{f,0}^\circ[\text{Cr}] + \Delta H_{f,0}^\circ[\text{F}^-] - \Delta H_{\text{rxn},0}^\circ \quad (15)$$

The HF, MP2, CCSD, and CCSD(T) energies given in Tables 5–7 were computed using the aug-cc-pVQZ or 6-311+G(3df) set on the halogen atoms and the Bauschlicher ANO basis on the transition metals. The employed geometries were the optimum B3LYP/6-311+G(d) structures, except for CrCl₂ and CrF₂, for which the CCSD(T)/6-311+G(d) structures were used. These geometries were employed for the computation of the corrections for the core-valence correlation and scalar relativistic effects also.

TABLE 5: Evaluation of $\Delta H_{f,0}^\circ$ and $\Delta H_{f,298.15}^\circ$ for Chromium Halides^a

	CrF rxn 1	CrF rxn 2	CrF ₂ rxn 3	CrCl rxn 4	CrCl rxn 5	CrCl ₂ rxn 6
$\Delta E_{\text{rxn}}[\text{HF}]$	50.15	114.23	233.15	7.07	44.75	102.78
$\delta[\text{MP2}]$	-20.58	-42.27	-72.18	-12.54	-24.70	-35.86
$\delta[\text{CCSD}]$	+7.15	+8.45	+7.85	+9.69	+13.70	+7.82
$\delta[\text{CCSD(T)}]$	-0.21	-3.58	-5.62	+0.38	-2.11	-3.86
$\delta[\text{core}]$	-1.33	-1.33	-2.63	-0.73	-0.73	-2.01
$\delta[\text{rel}]$	+2.80	+2.82	+3.23	+2.73	+2.58	+3.03
$\delta[\text{ZPVE}]$	-0.89	+0.51	+0.77	-0.54	+0.19	+0.21
$\Delta H_{\text{rxn},0}^\circ$	37.09	78.83	164.57	6.06	33.68	72.11
$\Delta H_{f,0}^\circ$	-2.53	-2.81	-107.02	33.61	32.22	-34.80
$\Delta H_{f,298.15}^\circ$	-2.59	-2.46	-106.71	33.84	32.40	-34.76

^a All entries in kcal mol^{-1} . $\Delta E_{\text{rxn}}[\text{HF}]$ is the computed reaction energy at the Hartree–Fock level of theory, and $\delta[\text{MP2}]$, $\delta[\text{CCSD}]$, and $\delta[\text{CCSD(T)}]$ each represent the increment in the reaction energy relative to the preceding level of theory. $\delta[\text{core}]$, $\delta[\text{rel}]$, and $\delta[\text{ZPVE}]$ denote the contributions from core-valence correlation, scalar relativistic effects, and zero-point vibrational energy. $\Delta H_{f,0}^\circ$ and $\Delta H_{f,298.15}^\circ$ are computed from $\Delta H_{\text{rxn},0}^\circ$ as described in the text.

TABLE 6: Evaluation of $\Delta H_{f,0}^\circ$ and $\Delta H_{f,298.15}^\circ$ for Manganese Halides^a

	MnF rxn 7	MnF ₂ rxn 8	MnCl rxn 9	MnCl ₂ rxn 10
$\Delta E_{\text{rxn}}[\text{HF}]$	81.64	201.65	73.54	131.14
$\delta[\text{MP2}]$	+38.17	+9.94	+16.99	+6.47
$\delta[\text{CCSD}]$	-13.68	-9.76	-8.95	-5.56
$\delta[\text{CCSD(T)}]$	+2.57	-1.06	+1.58	+0.00
$\delta[\text{core}]$	-1.90	-2.60	-1.24	-1.20
$\delta[\text{rel}]$	-1.80	-2.20	-1.84	-2.44
$\delta[\text{ZPVE}]$	-0.85	-0.82	-0.52	-0.61
$\Delta H_{\text{rxn},0}^\circ$	104.15	195.15	79.56	127.80
$\Delta H_{f,0}^\circ$	-18.26	-127.72	16.45	-60.39
$\Delta H_{f,298.15}^\circ$	-17.98	-127.70	16.46	-60.33

^a All entries in kcal mol^{-1} . See footnote of Table 5 for details.

TABLE 7: Evaluation of $\Delta H_{f,0}^\circ$ and $\Delta H_{f,298.15}^\circ$ for Iron Halides^a

	FeF rxn 11	FeF ₂ rxn 12	FeCl rxn 13	FeCl ₂ rxn 14
$\Delta E_{\text{rxn}}[\text{HF}]$	83.61	208.86	72.61	133.59
$\delta[\text{MP2}]$	+37.48	+8.66	+16.84	+6.53
$\delta[\text{CCSD}]$	-12.63	-8.76	-8.05	-4.74
$\delta[\text{CCSD(T)}]$	+2.60	-1.08	+1.67	+0.26
$\delta[\text{core}]$	-1.63	-2.17	-1.07	-0.83
$\delta[\text{rel}]$	-2.37	-3.24	-1.38 ^b	-1.30
$\delta[\text{ZPVE}]$	-0.90	-0.93	-0.54	-0.67
$\Delta H_{\text{rxn},0}^\circ$	106.16	201.34	80.08	132.84
$\Delta H_{f,0}^\circ$	11.04	-102.61	47.24	-34.11
$\Delta H_{f,298.15}^\circ$	11.04	-102.57	47.53	-34.79

^a All entries in kcal mol^{-1} . See footnote of Table 5 for details. ^b Computed using the (unmodified) Bauschlicher ANO set on Fe and the cc-pVTZ set on Cl; convergence problems for FeCl precluded the use of the basis sets employed for the other relativistic computations.

$\Delta H_{f,298.15}^\circ$ values were obtained using the computed $\Delta H_{f,0}^\circ$ values as well as the heats of formation in Table 3 and the thermal corrections computed at the B3LYP/6-311+G(d) level. For example, the $\Delta H_{f,298.15}^\circ[\text{CrF}]$ value from reaction 1 was computed from the expression

$$\Delta H_{f,298.15}^\circ = \Delta H_{f,0}^\circ[\text{CrF}] + \Delta H_{f,298.15}^\circ[\text{Cr}] - \Delta H_{f,0}^\circ[\text{Cr}] + \Delta H_{f,298.15}^\circ[\text{F}^-] - \Delta H_{f,0}^\circ[\text{F}^-] + H_{\text{Thermal}}[\text{CrF}] - H_{\text{Thermal}}[\text{Cr}] - H_{\text{Thermal}}[\text{F}^-] \quad (16)$$

where H_{Thermal} denotes the enthalpy difference, $H_{298.15}^\circ - H_0^\circ$.

Consider the chromium halides first, for which the computation of the heats of formation is given in Table 5. There is good agreement between the two values of -2.6 and -2.5 kcal mol $^{-1}$ that were determined for $\Delta H_{f,298.15}^{\circ}[\text{CrF}]$ from reactions 1 and 2. The dissociative electron attachment, reaction 1, converges somewhat faster with respect to the improvement of the level of electron correlation, having a CCSD \rightarrow CCSD(T) shift of only -0.21 kcal mol $^{-1}$. For the two reactions employed for CrCl, the dissociative electron attachment, reaction 4, also displays faster convergence with respect to the improvement of the level of theory; the computed values of 33.8 and 32.4 kcal mol $^{-1}$ for $\Delta H_{f,298.15}^{\circ}[\text{CrCl}]$ are in good agreement. For CrF and CrCl, we compute our best estimates as the average of the two numbers that were obtained for each species, and hence, we propose the values $\Delta H_{f,0}^{\circ}[\text{CrF}, \text{CrCl}] = [-2.7, 32.9]$ kcal mol $^{-1}$ and $\Delta H_{f,298.15}^{\circ}[\text{CrF}, \text{CrCl}] = [-2.5, 33.1]$ kcal mol $^{-1}$. For CrF $_2$ and CrCl, our $\Delta H_{f,298.15}^{\circ}$ values of -106.7 and 33.1 kcal mol $^{-1}$ agree well with the experimental values $\Delta H_{f,298.15}^{\circ}[\text{CrF}_2] = -103.23 \pm 2.96$ kcal mol $^{-1}$ and $\Delta H_{f,298.15}^{\circ}[\text{CrCl}] = 33.7 \pm 1.6$ and 31.05 ± 0.65 kcal mol $^{-1}$. For CrF and CrCl $_2$, however, our $\Delta H_{f,298.15}^{\circ}$ values of -2.5 and -34.8 kcal mol $^{-1}$ lie significantly below the experimental values of 4.57 ± 2.41 kcal mol $^{-1}$ for CrF $_2$ and -26.3 ± 1 and -28.11 ± 0.41 kcal mol $^{-1}$ for CrCl $_2$.^{3,2} Our $\Delta H_{f,0}^{\circ}[\text{CrF}]$ value of -2.7 kcal mol $^{-1}$ agrees very well with the value of $\Delta H_{f,0}^{\circ} = -3.1$ kcal mol $^{-1}$ previously computed at the CCSD(T) level using large basis sets and including corrections for relativistic effects and core correlation.²⁷ A value of 4 kcal mol $^{-1}$ for $\Delta H_{f,0}^{\circ}[\text{CrF}]$ (cf. Table 2) can be derived from the D_e value computed by Koukounas et al.³⁴ The D_e value was obtained at the MRCI level of theory, including the Davidson correction as well as corrections for core-correlation and scalar relativistic effects. Koukounas et al. also computed the D_e value at the CCSD(T) level, and the excellent agreement between the CCSD(T) result, $D_e = 113.5$ kcal mol $^{-1}$, and the Davidson corrected MRCI value of 113.3 kcal mol $^{-1}$ indicates that the disagreement between our $\Delta H_{f,0}^{\circ}[\text{CrF}]$ value and the value derived from D_e is not due to a deficiency in the single-reference CCSD(T) approach. Further investigations would be required to reveal the precise nature of this discrepancy, although it appears to be due mainly to differences in the computed relativistic corrections. For CrCl $_2$, a $\Delta H_{f,0}^{\circ}$ value of -29.5 kcal mol $^{-1}$ has been computed using density functional theory,³⁵ but no theoretical values using higher correlation models have been published previously.

For the manganese halides, all of the employed reactions display a fairly rapid convergence with improvement of the correlation treatment, with the difference between the CCSD and CCSD(T) reaction energies being about 2 kcal mol $^{-1}$ or less. Our computed $\Delta H_{f,298.15}^{\circ}$ values for MnF, MnF $_2$, MnCl, and MnCl $_2$ are -18.0 , -127.7 , 16.5 , and -60.3 kcal mol $^{-1}$, respectively. For MnCl and MnCl $_2$, the experimental values of 15.8 ± 1.6 and -62.6 ± 1 kcal mol $^{-1}$ reported in the literature³ agree well with our computed values. Although no experimental value is available for MnF $_2$, a $\Delta H_{f,298.15}^{\circ}[\text{MnF}]$ value of -5.2 kcal mol $^{-1}$ has been reported.⁵ On the basis of the agreement between the experiment and our computed values for the manganese chlorides and the convergence properties exhibited by reaction 7, we believe that the experimental value for the heat of formation of MnF is probably in error. Another high-level ab initio value for $\Delta H_{f,0}^{\circ}[\text{MnF}]$ can be obtained from the computations of $D_e[\text{MnF}]$ reported in the literature³⁴ (Table 2). Thus, a value of $\Delta H_{f,0}^{\circ}[\text{MnF}] = -19.5$ kcal mol $^{-1}$ can be computed from a D_e value of 106.5 kcal mol $^{-1}$ that was obtained

at the MRCI level employing large basis sets and including the Davidson correction as well as corrections for core-correlation and scalar relativistic effects. This value is in good agreement with our value, and the agreement between the Davidson corrected MRCI and the CCSD(T) D_e values reported in ref 34 suggests that the CCSD(T) method is adequate for MnF.

The reactions employed for the iron halides are analogous to those used for the manganese halides and display the same convergence patterns. Our computed $\Delta H_{f,298.15}^{\circ}$ values for the iron halides FeF, FeF $_2$, FeCl, and FeCl $_2$ are, in order, 11.0 , -102.6 , 47.5 , and -34.8 kcal mol $^{-1}$. For the chlorides, these values are in good agreement with the reported experimental $\Delta H_{f,298.15}^{\circ}$ values of 49.5 kcal mol $^{-1}$ for FeCl $_3$ and -33.7 ± 0.5 and -32.8 ± 1 kcal mol $^{-1}$ for FeCl $_2$.^{3,4} For FeF, our value agrees well with the experimental⁴ $\Delta H_{f,298.15}^{\circ}$ value of 11.4 ± 4.8 kcal mol $^{-1}$ also, but for FeF $_2$, the experimental $\Delta H_{f,298.15}^{\circ}$ value of -93.1 ± 3.4 kcal mol $^{-1}$ differs significantly from our value. A redetermination of the experimental heat of formation for FeF $_2$ would be useful in resolving this discrepancy. For FeF and FeCl, the bond dissociation energy D_0 has been computed previously³⁶ by employing the CCSD(T) method and using the Bauschlicher ANO basis set for Fe and the aug-cc-pVQZ set for F and Cl. The resulting D_0 values of 4.78 and 3.59 eV for FeF and FeCl, respectively, agree with our CCSD(T) values of 4.78 and 3.60 eV (cf. Table 7) before application of the corrections for core-correlation and scalar relativistic effects. The final values proposed in ref 36 were 4.91 and 3.73 eV for FeF and FeCl, respectively, obtained by including an empirical correction based on results computed for CuCl. Our final D_0 values of 4.61 and 3.47 kcal mol $^{-1}$ thus differ from those proposed in ref 36 by including corrections for core-correlation and relativistic effects and not including any empirical corrections.

For all of the investigated transition-metal halides, polynomial fits were made for the heat capacity (C_p), enthalpy (H°), and entropy (S°) as a function of temperature. Fits were performed over two separate temperature ranges, 300 – 1000 and 1000 – 3000 K, using C_p , H° , and S° values computed at 100 K intervals. These fits can be used with the CHEMKIN software package¹¹ and are defined by

$$\frac{C_p}{R} = a_1 + a_2 T + a_3 T^2 + a_4 T^3 + a_5 T^4 \quad (17)$$

$$\frac{H^\circ}{RT} = a_1 + \frac{a_2}{2} T + \frac{a_3}{3} T^2 + \frac{a_4}{4} T^3 + \frac{a_5}{5} T^4 + \frac{a_6}{T} \quad (18)$$

$$\frac{S^\circ}{R} = a_1 \ln T + a_2 T + \frac{a_3}{2} T^2 + \frac{a_4}{3} T^3 + \frac{a_5}{4} T^4 + a_7 \quad (19)$$

where $H^\circ = H^\circ(T) - H^\circ(298) + \Delta H_f^\circ(298)$, $\Delta H_f^\circ(298)$ is the species heat of formation at 298 K, $H^\circ(T)$ is the standard enthalpy at temperature T , and $H^\circ(298)$ is the standard enthalpy at 298 K. The fitted coefficients are available on the World Wide Web¹ and may also be obtained from the authors.

4. Concluding Remarks

Heats of formation of the transition-metal fluorides and chlorides MF $_n$ and MCl $_n$ (M = Cr, Mn, Fe; $n = 1, 2$) have been determined by high-level ab initio electronic-structure methods. Geometries and harmonic vibrational frequencies were computed at the B3LYP level of theory using triple- ζ basis sets including diffuse and polarization functions. Heats of formation were obtained from isogyric reaction energies at the CCSD(T)

level using high-quality basis sets and including corrections for core-valence correlation and scalar relativistic effects. Because of the previous uncertainty regarding the structure of the global minimum on the CrF₂ and CrCl₂ potential energy surfaces, geometry optimizations were performed at both the B3LYP and CCSD(T) levels for these species. At both levels, a bent (⁵B₂) minimum was located, and the linear form was found to be a transition state only slightly higher in energy. Our computed heats of formation provide a consistent set of ab initio data for the investigated transition-metal halides and fill the gaps in the available experimental data for these compounds. Although several of the published experimental heats of formation are corroborated by our computed values, our results suggest that some of the previously determined experimental heats of formation may be in error. For all of the investigated transition-metal halides, polynomial fits were carried out for the heat capacity and the standard enthalpy and entropy in the 300–1000 and 1000–3000 K temperature ranges.

5. Acknowledgments

This work was supported in part by the U.S. Department of Energy (DOE) Industrial Technologies Program: Industrial Materials for the Future Program.

References and Notes

- http://www.ca.sandia.gov/HiTempThermo/.
- Ebbinghaus, B. B. *Combust. Flame* **1995**, *101*, 311.
- Hildenbrand, D. L. *J. Chem. Phys.* **1995**, *103*, 2634.
- Chase, M. W.; et al. JANAF Thermochemical Tables, 3rd ed. *J. Phys. Chem. Ref. Data* **1985**, *14* (Suppl. 1).
- Wagman, D. D.; et al. NBS Tables of Chemical Thermodynamic Properties. *J. Phys. Chem. Ref. Data* **1982**, *11* (Suppl. 2).
- Hargittai, M. *Coord. Chem. Rev.* **1988**, *91*, 35.
- Hargittai, M.; Dorofeeva, O. V.; Tremmel, J. *Inorg. Chem.* **1985**, *24*, 3963.
- Bridgeman, A. J.; Bridgeman, C. H. *Chem. Phys. Lett.* **1997**, *272*, 173.
- Jensen, V. R. *Mol. Phys.* **1997**, *91*, 131.
- Zasorin, E. Z.; Gershikov, A. G.; Spiridonov, V. P.; Ivanov, A. A. *J. Struct. Chem.* **1988**, *28*, 680.
- Kee, R. J.; Rupley, F. M.; Miller, J. A.; Coltrin, M. E.; Grcar, J. F.; Meeks, E.; Moffat, H. K.; Lutz, A. E.; Dixon-Lewis, G.; Smooke, M. D.; Warnatz, J.; Evans, G. H.; Larson, R. S.; Mitchell, R. E.; Petzold, L. R.; Reynolds, W. C.; Caracotsios, M.; Stewart, W. E.; Glarborg, P.; Wang, C.; Adignun, O. *Chemkin Collection*, Release 3.6 ed.; Reaction Design, Inc.: San Diego, CA, 2000.
- Frisch, M. J.; Pople, J. A.; Binkley, J. S. *J. Chem. Phys.* **1984**, *80*, 3265.
- Bauschlicher, C. W. *Theor. Chim. Acta* **1995**, *92*, 183.
- Obtained from the Extensible Computational Chemistry Environment Basis Set Database, Version 1/02/02, as developed and distributed by the Molecular Science Computing Facility, Environmental and Molecular Sciences Laboratory which is part of the Pacific Northwest Laboratory, P.O. Box 999, Richland, WA 99352, USA, and funded by the U.S. Department of Energy. The Pacific Northwest Laboratory is a multiprogram laboratory operated by Battelle Memorial Institute for the U.S. Department of Energy under Contract DE-AC06-76RLO 1830. Contact David Feller or Karen Schuchardt for further information.
- Dunning, T. H., Jr. *J. Chem. Phys.* **1989**, *90*, 1007.
- Woon, D. E.; Dunning, T. H., Jr. *J. Chem. Phys.* **1993**, *98*, 1358.
- Kendall, R. A.; Dunning, T. H., Jr.; Harrison, R. J. *J. Chem. Phys.* **1992**, *96*, 6796.
- Douglas, M.; Kroll, N. M. *Ann. Phys. (NY)* **1974**, *82*, 89.
- Hess, B. A. *Phys. Rev. A: At., Mol., Opt. Phys.* **1985**, *32*, 756.
- Hess, B. A. *Phys. Rev. A: At., Mol., Opt. Phys.* **1986**, *33*, 3742.
- Jansen, G.; Hess, B. A. *Phys. Rev. A: At., Mol., Opt. Phys.* **1989**, *39*, 6016.
- de Jong, W. A.; Harrison, R. J.; Dixon, D. A. *J. Chem. Phys.*, unpublished work.
- (a) These optimizations were performed with the Molpro UCCSD(T) method, which uses a high-spin RHF wave-function reference. (b) Amos, R. D.; Bernhardtsson, A.; Berning, A.; Celani, P.; Cooper, D. L.; Deegan, M. J. O.; Dobbyn, A. J.; Eckert, F.; Hampel, C.; Hetzer, G.; Knowles, P. J.; Korona, T.; Lindh, R.; Lloyd, A. W.; McNicholas, S. J.; Manby, F. R.; Meyer, W.; Mura, M. E.; Nicklass, A.; Palmieri, P.; Pitzer, R.; Rauhut, G.; Schütz, M.; Schumann, U.; Stoll, H.; Stone, A. J.; Tarroni, R.; Thorsteinsson, T.; Werner, H.-J. *MOLPRO*, a package of ab initio programs designed by H.-J. Werner and P. J. Knowles, version 2002.3.
- (a) Straatsma, T. P.; Aprà, E.; Windus, T. L.; Bylaska, E. J.; de Jong, W.; Hirata, S.; Valiev, M.; Hackler, M.; Pollack, L.; Harrison, R.; Dupuis, M.; Smith, D. M. A.; Nieplocha, J.; Tipparaju V.; Krishnan, M.; Auer, A. A.; Brown, E.; Cisneros, G.; Fann, G.; Früchtl, H.; Garza, J.; Hirao, K.; Kendall, R.; Nichols, J.; Tsemekhan, K.; Wolinski, K.; Anchell, J.; Bernholdt, D.; Borowski, P.; Clark, T.; Clerc, D.; Dachsel, H.; Deegan, M.; Dyall, K.; Elwood, D.; Glendenning, E.; Gutowski, M.; Hess, A.; Jaffe, J.; Johnson, B.; Ju, J.; Kobayashi, R.; Kutteh, R.; Lin, Z.; Littlefield, R.; Long, X.; Meng, B.; Nakajima, T.; Niu, S.; Rosing, M.; Sandrone, G.; Stave, M.; Taylor, H.; Thomas, G.; van Lenthe, J.; Wong, A.; Zhang, Z.; *NWChem, A Computational Chemistry Package for Parallel Computers*, Version 4.6; Pacific Northwest National Laboratory, Richland, WA 99352-0999, USA, 2004. (b) Kendall, R. A.; Aprà, E.; Bernholdt, D. E.; Bylaska, E. J.; Dupuis, M.; Fann, G. I.; Harrison, R. J.; Ju, J.; Nichols, J. A.; Nieplocha, J.; Straatsma, T. P.; Windus, T. L.; Wong, A. T. High Performance Computational Chemistry: an Overview of NWChem a Distributed Parallel Application, *Comput. Phys. Commun.* **2000**, *128*, 260–283.
- Frisch, M. J.; Trucks, G. W.; Schlegel, H. B.; Scuseria, G. E.; Robb, M. A.; Cheeseman, J. R.; Zakrzewski, V. G.; Montgomery, J. A., Jr.; Stratmann, R. E.; Burant, J. C.; Dapprich, S.; Millam, J. M.; Daniels, A. D.; Kudin, K. N.; Strain, M. C.; Farkas, O.; Tomasi, J.; Barone, V.; Cossi, M.; Cammi, R.; Mennucci, B.; Pomelli, C.; Adamo, C.; Clifford, S.; Ochterski, J.; Petersson, G. A.; Ayala, P. Y.; Cui, Q.; Morokuma, K.; Malick, D. K.; Rabuck, A. D.; Raghavachari, K.; Foresman, J. B.; Cioslowski, J.; Ortiz, J. V.; Stefanov, B. B.; Liu, G.; Liashenko, A.; Piskorz, P.; Komaromi, I.; Gomperts, R.; Martin, R. L.; Fox, D. J.; Keith, T.; Al-Laham, M. A.; Peng, C. Y.; Nanayakkara, A.; Gonzalez, C.; Challacombe, M.; Gill, P. M. W.; Johnson, B. G.; Chen, W.; Wong, M. W.; Andres, J. L.; Head-Gordon, M.; Replogle, E. S.; Pople, J. A. *Gaussian 98*, revision A.6; Gaussian, Inc.: Pittsburgh, PA, 1998.
- Frisch, M. J.; Trucks, G. W.; Schlegel, H. B.; Scuseria, G. E.; Robb, M. A.; Cheeseman, J. R.; Montgomery, J. A., Jr.; Vreven, T.; Kudin, K. N.; Burant, J. C.; Millam, J. M.; Iyengar, S. S.; Tomasi, J.; Barone, V.; Mennucci, B.; Cossi, M.; Scalmani, G.; Rega, N.; Petersson, G. A.; Nakatsuji, H.; Hada, M.; Ehara, M.; Toyota, K.; Fukuda, R.; Hasegawa, J.; Ishida, M.; Nakajima, T.; Honda, Y.; Kitao, O.; Nakai, H.; Klene, M.; Li, X.; Knox, J. E.; Hratchian, H. P.; Cross, J. B.; Adamo, C.; Jaramillo, J.; Gomperts, R.; Stratmann, R. E.; Yazyev, O.; Austin, A. J.; Cammi, R.; Pomelli, C.; Ochterski, J. W.; Ayala, P. Y.; Morokuma, K.; Voth, G. A.; Salvador, P.; Dannenberg, J. J.; Zakrzewski, V. G.; Dapprich, S.; Daniels, A. D.; Strain, M. C.; Farkas, O.; Malick, D. K.; Rabuck, A. D.; Raghavachari, K.; Foresman, J. B.; Ortiz, J. V.; Cui, Q.; Baboul, A. G.; Clifford, S.; Cioslowski, J.; Stefanov, B. B.; Liu, G.; Liashenko, A.; Piskorz, P.; Komaromi, I.; Martin, R. L.; Fox, D. J.; Keith, T.; Al-Laham, M. A.; Peng, C. Y.; Nanayakkara, A.; Challacombe, M.; Gill, P. M. W.; Johnson, B.; Chen, W.; Wong, M. W.; Gonzalez, C.; Pople, J. A. *Gaussian 03*, revision A.1; Gaussian, Inc.: Pittsburgh, PA, 2003.
- Espelid, Ø.; Børve, K. J. *J. Phys. Chem. A* **1997**, *101*, 9449.
- Vogt, N. *J. Mol. Struct.* **2001**, *570*, 189.
- Koivisto, R.; Launila, O.; Schimmelfennig, B.; Simard, B.; Wahlgren, U. *J. Chem. Phys.* **2001**, *114*, 8855.
- Launila, O. *J. Mol. Spectrosc.* **1995**, *169*, 373.
- Bencheikh, M.; Koivisto, R.; Launila, O.; Flament, J. P. *J. Chem. Phys.* **1997**, *106*, 6231.
- Blinova, O. V.; Shklyarik, V. G.; Shcherba, L. D. *Russ. J. Phys. Chem. (Engl. Transl.)* **1988**, *62*, 831.
- Hastie, J. W.; Hauge, R. H.; Margrave, J. L. *High Temp. Sci.* **1971**, *3*, 257.
- Koukounas, C.; Kardahakis, S.; Mavridis, A. *J. Chem. Phys.* **2004**, *120*, 11500.
- Wang, S. G.; Schwarz, W. H. E. *J. Chem. Phys.* **1998**, *109*, 7252.
- Bauschlicher, C. W. *Chem. Phys.* **1996**, *211*, 163.
- Kent, R. A.; Margrave, J. L. *J. Am. Chem. Soc.* **1965**, *87*, 3582.
- Devore, T. C.; Gole, J. L. *J. Phys. Chem.* **1996**, *100*, 5660.
- Balducci, G.; Campodonico, M.; Gigli, G.; Meloni, G.; Cesaro, S. N. *J. Chem. Phys.* **2002**, *117*, 10613.
- Kent, R. A.; Ehlert, T. C.; Margrave, J. L. *J. Am. Chem. Soc.* **1964**, *86*, 5090.
- Schröder, D.; Loos, J.; Schwarz, H.; Thissen, R.; Dutuit, O. *Inorg. Chem.* **2001**, *40*, 3161.
- Kellogg, C. B.; Irikura, K. K. *J. Phys. Chem. A* **1999**, *103*, 1150.
- Bach, R. D.; Shobe, D. S.; Schlegel, H. B.; Nagel, C. J. *J. Phys. Chem. A* **1996**, *100*, 8770.
- Glukhovtsev, M. N.; Bach, R. D.; Nagel, C. J. *J. Phys. Chem. A* **1997**, *101*, 316.
- (45) *CRC Handbook of Chemistry and Physics*, 84th ed.; CRC Press: Boca Raton, FL, 2003.